



# Corn Starch-Based Bionanocomposite Film Reinforced With ZnO Nanoparticles and Different Types of Plasticizers

Heni Radiani Arifin<sup>1</sup>, Mohamad Djali<sup>1</sup>, Bambang Nurhadi<sup>1\*</sup>, Shafrina Azlin-Hasim<sup>2</sup>, Nanang Masruchin<sup>3</sup>, P. Almira Vania<sup>1</sup> and Amani Hilmi<sup>1</sup>

<sup>1</sup> Department of Food Industrial Technology, Universitas Padjadjaran, Bandung, Indonesia, <sup>2</sup> Faculty of Fisheries and Food Science, Universiti Malaysia Terengganu, Kuala Terengganu, Malaysia, <sup>3</sup> Research Center for Biomaterials, Indonesia Institute of Science (LIPI), Cibinong, Indonesia

## OPEN ACCESS

### Edited by:

Benny Tjahjono,  
Coventry University, United Kingdom

### Reviewed by:

Asad Mohammad Amini,  
University of Kurdistan, Iran  
Felycia Edi Soetaredjo,  
Universitas Katolik Widya Mandala  
Surabaya, Indonesia

### \*Correspondence:

Bambang Nurhadi  
bambang.nurhadi@unpad.ac.id

### Specialty section:

This article was submitted to  
Sustainable Food Processing,  
a section of the journal  
Frontiers in Sustainable Food Systems

Received: 28 February 2022

Accepted: 30 May 2022

Published: 13 July 2022

### Citation:

Arifin HR, Djali M, Nurhadi B, Azlin-Hasim S, Masruchin N, Vania PA and Hilmi A (2022) Corn Starch-Based Bionanocomposite Film Reinforced With ZnO Nanoparticles and Different Types of Plasticizers. *Front. Sustain. Food Syst.* 6:886219. doi: 10.3389/fsufs.2022.886219

Corn starch var. Paragon from Indonesia and carboxymethyl cellulose (CMC) were used to develop bionanocomposite film containing different types of plasticizers [glycerol (G) or sorbitol (S)] incorporated with zinc oxide (ZnO) nanoparticles (NPs) (0, 3, 5 wt.%) via casting method. The main objective of this study was to improve the properties of the bionanocomposite film with incorporated different types of plasticizers and ZnO NPs. The physicochemical properties of the film were systematically characterized. The results showed that the incorporation of sorbitol could significantly enhance the value of tensile strength, elongation, and Young's modulus than glycerol. In general, a higher concentration of ZnO NPs in the film could increase the tensile strength, reduce the water vapor permeability, decrease the water solubility, and influence the morphology, crystallinity, functional groups, and thermal stability of the films. The data showed that corn starch bionanocomposite film containing sorbitol with 5 wt% ZnO NPs was the most optimal film as compared to other formulations as the solubility and water vapor transmission rate (WVTR) value significantly reduced, and also it increased the value of tensile strength, elongation, and Young's modulus. It can be concluded that the incorporation of glycerol or sorbitol plasticizers reinforced by ZnO NPs plays an important role in improving the properties of bionanocomposite film, hence the film has the potency to be used as sustainable and environmental friendly packaging.

**Keywords:** sorbitol, glycerol, zinc oxide nanoparticles, corn starch, bionanocomposite film

## INTRODUCTION

Among the biopolymers, corn starch contains hydrocolloid components that can be utilized to form a nanocomposite film matrix. In general, corn starch has high amylose content, about 25% (w/w), allowing it to produce a strong film (Tavares et al., 2019). The utilization of corn starch var. Paragon has the potential to be used as a film matrix polymer. However, this corn starch-based biodegradable film has several drawbacks: rigidity, brittleness, and high hygroscopic properties resulting in poor physical and mechanical properties (Isotton et al., 2015). In addition, starch-based films have low moisture barrier properties (de Melo et al., 2011). These limitations

can be overcome by incorporating nanofillers into the polymer matrix and controlling the mechanical properties and film permeability (Montero et al., 2017; Hu et al., 2019). The results of previous research reported that bionanocomposite films can significantly improve the mechanical properties, resistance to water vapor and gasses, and stable dimensions compared to polymers without nanofillers (Sadegh-Hassani and Mohammadi Nafchi, 2014; Babaei-Ghazvini et al., 2018; Vaezi et al., 2019).

Zinc oxide (ZnO) is one of the oxide group compounds that is widely used as a source of nanoparticles. Generally, ZnO nanoparticles (ZnO NPs) have been widely used in various applications, such as packaging, cosmetics, pharmaceuticals, dye degradation, optical devices, and biosensors (Liu et al., 2019). In recent years, the use of ZnO NPs as filler nanocomposite in bioplastic films has been growing because of its strong ability to interact with the polymer matrix to produce nanocomposite films with better physical, mechanical, chemical, and biological properties than the bulk form (Vaezi et al., 2019). ZnO is currently one of the five zinc compounds listed as a generally recognized safe (GRAS) material.

Despite its excellent properties, Arifin et al. (2022) reported that nanocomposite films made from starch-CMC with the addition of ZnO nanoparticles still have a rigid and brittle film quality, so it is necessary to add additives that act as plasticizers to increase the plastic properties of the film. Plasticizers are often used to improve elasticity and reduce the barrier film properties of starch (Gontard et al., 1993). Some of the plasticizers that can be used are glycerol and sorbitol. Febrianto Mulyadi et al. (2016) stated that glycerol could reduce intermolecular strength and increase flexibility and extensibility of the film to produce a good mechanical quality film. Meanwhile, according to Astuti (2011), sorbitol could reduce internal hydrogen bonds in intermolecular bonds of the film so that it could inhibit the evaporation of water from the product which was packaged (instant noodle seasoning). It can enter each polymer chain so that it will facilitate the movement of polymer molecules in film products. Recent reports have shown that the application of ZnO NPs to biopolymers could reduce the hydrophilic properties, as well as improve the mechanical properties and film permeability (Mohammadi Nafchi et al., 2014; Marvizadeh et al., 2017; Hu et al., 2019). To the best of our knowledge, there are no reports of ZnO NPs in biopolymer systems combined with various plasticizers, so this work aims to evaluate the properties of nanocomposite films incorporated with ZnO NPs containing plasticizers (glycerol or sorbitol) with corn starch as polymer base.

## MATERIALS AND METHODS

### Materials

A local farmer supplied the corn kernel var. Paragon (Indonesia). ZnO NPs (202.9 nm) were milled with ball milling performed at PRINT-G Unpad. The materials of glycerol, sorbitol, carboxymethyl cellulose (CMC) (Blanose France brand), filter paper (Whatman no. 40), PP plastic (Bangkuang brand), and silica gel (Wonder Natural brand) were purchased from Bratachem, Indonesia.

### Corn Starch Extraction

Corn starch was extracted according to Marta et al. (2019) with slight modifications. A total of 500 g of corn kernels were milled in a blender with 500 ml of water. The corn starch slurry was filtered and squeezed several times while aquadest was added, then the corn dregs were removed and the starch suspension was precipitated for 24 h. The clear filtrate was discarded and the starch precipitate with a little aquadest was centrifuged at 4,000 rpm for 15 min to separate the wet starch from the filtrate. Wet starch had been dried in an oven at 50°C for 12 h. A grinder was used to crush the dried starch. To obtain homogeneous and fine-grained starch, sieving was done with an 80-mesh sieve.

### Bionanocomposite Film Preparation

The bionanocomposite film preparation method was prepared according to Arifin et al. (2022) with minor modifications. A total of 7 g of corn starch was mixed with 200 ml of distilled water to produce a 3.5% (w/v) corn starch solution. Meanwhile, ZnO NPs were dispersed in distilled water. After that, CMC (0.5% w/v) was added to the corn solution while stirring constantly. After the CMC dissolved, the dispersed ZnO NPs (0, 3, or 5 wt. %) were added. The mixture was then stirred in a beaker glass fitted with a magnetic bar and heated on a hot plate stirrer. After reaching the temperature of corn starch gelatinization (62°C), 2% (v/v) plasticizer glycerol or sorbitol plasticizer was added. Then, the film solution was heated to 70°C and continuously stirred. The solution was then cooled to around 40°C. The formation of films was conducted by pouring 160 ml film solution into a 20 cm x 20 cm mold. The film plate was dried at 50°C for 24 h.

### Film Color

Spectrophotometer CM 5 (Konica Minolta Co., Osaka, Japan) with Spectra Magic software was used to measure the color.  $L^*$  (lightness, 0 = black/100 = white),  $a^*$  ( $+a^*$  = redness/ $-a^*$  = greenness),  $b^*$  ( $+b^*$  = yellowness/ $-a^*$  = blueness), and hue are all part of the color measurement. Calibration was carried out using a zero-calibration plate (CM-A124) and a white calibration plate (CM-A120) with a large target mask (CM-A203). The film was placed on the transmittance specimen holder, and the rays were shot at two different parts (Schanda, 2007).

### Film Thickness

The thickness was measured using a micrometer screw. The film was measured in all four corners and the center. For each sample, the average of five measurements was calculated (Kanmani and Rhim, 2014). The thickness was specified in millimeters, and the micrometer screw used has an accuracy of 0.01 mm.

### Moisture Content

The moisture content of bionanocomposite films was measured using a thermogravimetric method described by AOAC (2005). The principle of this method was based on the evaporation of water present in the material by heating and then weighed to a constant weight. The weight reduction that occurs is the water content contained in the ingredients.

## Water Solubility

Water solubility was assessed by a procedure described by Kotharangannagari and Krishnan (2016). In distilled water, rectangular (a) and filter paper (b) cut samples were immersed. The samples were filtered through filter paper after 24 h of agitation (250 rpm) in 50 mL distilled water at 25°C. The filter paper was then dried at 105°C for 24 h to obtain the final dry weight (c), and the film solubility (percent) was determined using the equation:

$$\text{Percent of solubility} = \frac{a - (c - b)}{a} \times 100\% \quad (1)$$

where a = initial sample weight (g), b = filter paper weight (g), c = dry weight of filter paper and samples (g).

## Water Vapor Transmission Rate

The water vapor transmission rate was calculated according to ASTM E96 (ASTM, 2005). The film sample to be tested was sealed in a cup containing 10 g of silica gel (RH = 0%). The cups were then placed at 25°C in a jar containing 40% (w/v) saturated NaCl salt solution (RH = 75%). For 8 h, the weight of the cups was measured every hour, and the weight loss from each cup was calculated. The water vapor transmission rate (WVTR) was calculated using the slopes (linear) of the steady-state portion of the cup's weight loss vs. the time curve. As a result, the linear line's slope was calculated as water vapor absorption per hour (g/h). The following formula was used to calculate WVTR:

$$\text{WVTR} = \frac{\text{slope}}{A} \quad (2)$$

where WVTR = water vapor transmission rate (g/m<sup>2</sup>.h), slope = absorption of moisture every hour (g/h), A = film area (m<sup>2</sup>).

## Mechanical Properties

Mechanical properties testing was performed in accordance with ASTM (ASTM, 2002). The Universal Testing Machine Brand SHIMADZU AG IS, Japan used a tool with a load cell of 1 kN and a speed of 10 mm/min. The films were conditioned for more than 40 h before testing in a room at 23°C and 50 % RH. Tensile strength was determined by the maximum load applied when the film was torn, whereas the proportion of elongation was determined by the increase in film length at the break. Meanwhile, Young's modulus was determined by dividing the tensile strength by the percentage elongation.

## Scanning Electron Microscope

The morphology film was examined with a JEOL JSM-6360LA Scanning Electron Microscope (Japan). A thin film was frozen in liquid nitrogen before being fractured, mounted in a special holder, gold-coated, and examined. The sample was folded at 90° for inspection while being analyzed in cross-section (Vaezi et al., 2019).

## X-Ray Diffraction

The X-ray diffraction pattern of the film was measured using a MiniFlex XRD system delivery speed and sensitivity through

innovative technology advances, including the HyPix-400 MF 2D hybrid pixel array detector (HPAD) together with an available 600 W X-ray source and new 8-position automatic sample changer. The diffraction angle scanning ranged from 3 to 90° with a scan speed of 10 deg/min and a step width of 0.02° (Marta et al., 2019). A thin film was placed on the surface of the plate holder for measuring the diffraction angle.

## Fourier Transform Infrared

The FTIR spectrophotometer (Thermo Scientific® Nicolet iS5 with detector DGTS (Deuterated Triglycine Sulfate), ZnSe iD3 ATR Holder) was used to record the film spectrum in reflection mode (total attenuated reflection). The wave absorption was measured after a thin film was placed on the surface of the FTIR holder (Marvzadeh et al., 2017).

## Thermogravimetric Analysis/Derivative Thermogravimetric

The thermal stability of the film was determined using a TGA 4000 (Perkin Elmer, United States). The amount sample was heated from room temperature to 600°C at a rate of 10°C min<sup>-1</sup> under a nitrogen flow atmosphere (50 ml/min). The derivative thermogravimetric (DTG) curve was expressed as the mass variation as a function of temperature (Nurhadi et al., 2021).

## Statistical Analysis

The data were analyzed using univariate analysis of variance (ANOVA) in SPSS 19.0 statistical software program to compare plasticizers type and ZnO NPs concentrations in nanocomposite film, and the least significant difference (LSD) comparison test was used to determine the significant difference between treatments at a significance level of 5% (P.05).

## RESULTS

### Mechanical Properties

The tensile strength of the film ranged from 0.74 to 6.07 MPa (Table 1), and this complied with the JIS (1975) where the minimum value was 0.392 MPa. The value of the tensile strength of sorbitol-plasticized film was significantly higher than glycerol-plasticized film regardless of any concentration of ZnO NPs used. No significant difference in the value of tensile strength was observed when different concentrations of ZnO NPs were incorporated into glycerol-plasticized film. Furthermore, in the sorbitol-plasticized film, the addition of 3 and 5% ZnO NPs was significantly higher than 0% ZnO NPs.

The elongation at the break value of the film samples was around 29.74–117.92% (Table 1). Almost all treatments fit the Japanese Industrial Standard (1975), namely elongation values above 50% were considered to have good properties, except for the glycerol-plasticized film without ZnO NPs. The elongation at the break value of the sorbitol-plasticized film was significantly higher than the glycerol-plasticized film, regardless of the concentration of the ZnO NPs added.

The value of Young's modulus of films ranged from 0.10 to 0.57 MPa (Table 1). In general, the young modulus of the

**TABLE 1** | The tensile strength, elongation at break, and Young's modulus of bionanocomposite films.

Treatments	Tensile strength (MPa)	Elongation at break (%)	Young's modulus (MPa)
G + 0% ZnO NPs	0.74 ± 0.08 <sup>a</sup>	29.74 ± 6.19 <sup>a</sup>	0.025 ± 0.003 <sup>b</sup>
G + 3% ZnO NPs	0.85 ± 0.00 <sup>a</sup>	82.19 ± 4.73 <sup>c</sup>	0.010 ± 0.001 <sup>a</sup>
G + 5% ZnO NPs	0.79 ± 0.06 <sup>a</sup>	52.67 ± 9.48 <sup>b</sup>	0.015 ± 0.002 <sup>a</sup>
S + 0% ZnO NPs	4.11 ± 0.88 <sup>b</sup>	92.42 ± 6.52 <sup>c</sup>	0.044 ± 0.006 <sup>c</sup>
S + 3% ZnO NPs	5.36 ± 0.19 <sup>c</sup>	94.93 ± 6.21 <sup>c</sup>	0.057 ± 0.006 <sup>d</sup>
S + 5% ZnO NPs	6.07 ± 0.49 <sup>c</sup>	117.92 ± 5.96 <sup>d</sup>	0.051 ± 0.002 <sup>cd</sup>

The mean value of treatment denoted by the same letter indicates no significant difference at the 5% test level according to the LSD test. G, Glycerol; S, Sorbitol; ZnO NPs, Zinc oxide nanoparticles.

**TABLE 2** | The thickness, water-solubility, WVTR, and moisture content of bionanocomposite films.

Treatments	Thickness (mm)	Water solubility (%)	WVTR (g/m <sup>2</sup> .h)	Moisture content (%)
G + 0% ZnO NPs	0.260 ± 0.000 <sup>d</sup>	36.84 ± 0.41 <sup>c</sup>	9.64 ± 0.29 <sup>d</sup>	11.11 ± 0.40 <sup>c</sup>
G + 3% ZnO NPs	0.282 ± 0.001 <sup>e</sup>	33.26 ± 0.04 <sup>ab</sup>	6.20 ± 0.28 <sup>bc</sup>	10.93 ± 1.76 <sup>c</sup>
G + 5% ZnO NPs	0.283 ± 0.002 <sup>e</sup>	33.38 ± 0.56 <sup>b</sup>	5.15 ± 1.13 <sup>b</sup>	9.61 ± 0.38 <sup>b</sup>
S + 0% ZnO NPs	0.181 ± 0.001 <sup>a</sup>	32.12 ± 0.31 <sup>ab</sup>	8.24 ± 2.2 <sup>cd</sup>	8.29 ± 0.11 <sup>ab</sup>
S + 3% ZnO NPs	0.205 ± 0.006 <sup>b</sup>	32.76 ± 0.16 <sup>ab</sup>	4.58 ± 0.01 <sup>ab</sup>	7.84 ± 0.00 <sup>a</sup>
S + 5% ZnO NPs	0.224 ± 0.001 <sup>c</sup>	31.69 ± 1.60 <sup>a</sup>	2.85 ± 0.25 <sup>a</sup>	7.77 ± 0.15 <sup>a</sup>

The mean value of treatment denoted by the same letter indicates no significant difference at the 5% test level according to the LSD test. G, Glycerol; S, Sorbitol; ZnO NPs, Zinc oxide nanoparticles.

glycerol-plasticized film was significantly lower than the sorbitol-plasticized film regardless of any ZnO NPs concentrations used. Results showed that the value of the young modulus in the glycerol-plasticized film with the incorporation of 3 and 5% ZnO NPs was significantly lower than without the addition of ZnO NPs. Meanwhile, in the sorbitol-plasticized film, the addition of 3 and 5% ZnO NPs was significantly higher than the film without ZnO NPs on Young's modulus of films.

## Permeability of Films

The results showed that the WVTR value of the film ranged from 2.85 to 9.64 g/m<sup>2</sup> h (Table 2). This WVTR value complied with the standard determined by the Japanese Industrial Standard (1975) which was <10 g/m<sup>2</sup> h. In general, the WVTR values of sorbitol-plasticized films were significantly lower than those of glycerol-plasticized films, both at concentrations of 3% and 5% ZnO NPs. Meanwhile, the glycerol-plasticized film of 3 and 5% ZnO NPs were not significantly different, but the two treatments were significantly lower than the film without the addition of ZnO NPs. Furthermore, the WVTR value of sorbitol-plasticized film with the incorporation of 3 and 5% ZnO NPs was significantly lower than the control film (without the addition of ZnO NPs).

## Physical Properties







The solubility of nanocomposite films in water ranged from 31.69 to 36.84% (Table 2). In general, films with the addition of ZnO NPs showed a significant decrease in solubility than the glycerol-plasticized films without the addition of ZnO NPs.

The thickness of glycerol-plasticized film was significantly higher than sorbitol-plasticized film regardless of any concentration of ZnO NPs used (Table 2). In general, the thickness for both of the plasticized films (glycerol or sorbitol) significantly increased with the increase of ZnO NPs, except for glycerol with 5% ZnO NPs.

In general, the moisture content for both of the plasticized films (glycerol or sorbitol) significantly decreased with the increase of ZnO NPs. The moisture content of the glycerol-plasticized film with 0 and 3% ZnO NPs was significantly higher than the others (Table 2). Meanwhile, the moisture content of glycerol-plasticized film with 5% ZnO NPs was significantly different from sorbitol-plasticized film with 3 and 5% ZnO NPs and not significantly different from sorbitol-plasticized film with 0% ZnO NPs.

Based on Table 3, the L\* value of both glycerol or sorbitol-plasticized film without the presence of ZnO NPs was not significantly different; however, it was significantly higher than other film treatments containing ZnO NPs (3% or 5%). The results showed that a\* values ranged from 0.30 to 0.76, and this indicated that the color of the nanocomposite films tended to be redder. The color of a\* values of glycerol- or sorbitol-plasticized films without ZnO NPs were significantly different from 3 and 5% ZnO NPs. Meanwhile, the glycerol-/sorbitol-plasticized film with 5% ZnO NPs was significantly higher than the other treatments. The +b\* color value obtained ranges from 3.54 to 12.30, indicating that the color tended to be yellower. The yellowish color of the bionanocomposite films can be seen as a photograph in Figure 1. The b\* value

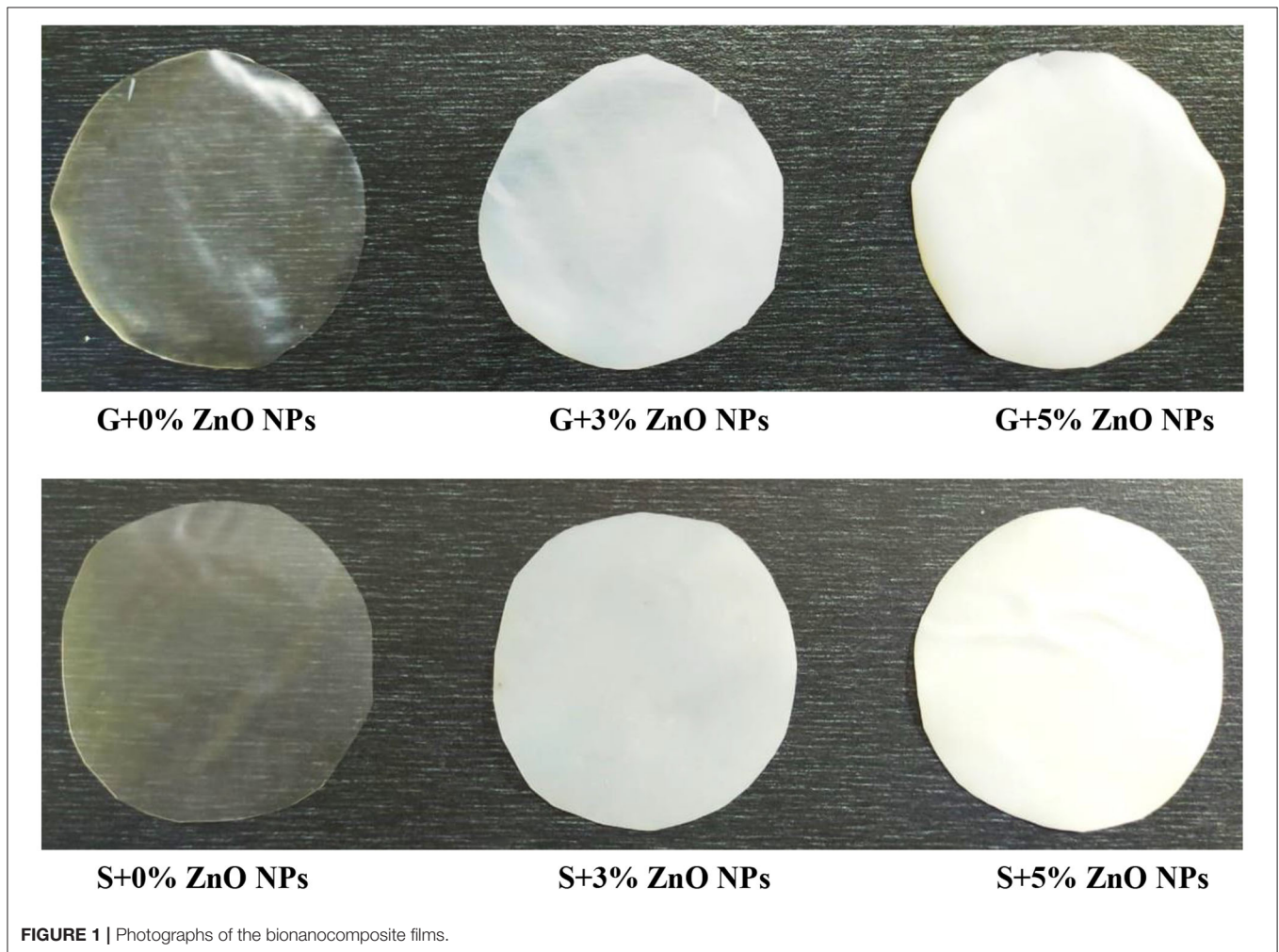
**TABLE 3** | The  $L^*$ ,  $a^*$ , and  $b^*$  value of bionanocomposite films.

Treatments	Image color films	$L^*$	$a^*$	$b^*$
G + 0% ZnO NPs		$97.69 \pm 0.21^c$	$0.30 \pm 0.06^{ab}$	$3.54 \pm 0.04^b$
G + 3% ZnO NPs		$77.61 \pm 5.04^a$	$0.56 \pm 0.08^c$	$12.30 \pm 0.41^e$
G + 5% ZnO NPs		$79.70 \pm 3.41^a$	$0.68 \pm 0.01^d$	$11.27 \pm 0.25^d$
S + 0% ZnO NPs		$98.49 \pm 0.40^c$	$0.19 \pm 0.05^a$	$1.66 \pm 0.01^a$
S + 3% ZnO NPs		$87.55 \pm 3.82^b$	$0.43 \pm 0.09^{bc}$	$10.44 \pm 0.33^c$
S + 5% ZnO NPs		$82.69 \pm 0.64^{ab}$	$0.76 \pm 0.04^d$	$11.05 \pm 0.01^d$

The mean value of treatment denoted by the same letter indicates no significant difference at the 5% test level according to the LSD test.

G, Glycerol; S, Sorbitol; ZnO NPs, Zinc oxide nanoparticles.

$L^*$ , chromatic brightness;  $a^*$ , chromatic green-red color;  $b^*$ , chromatic blue-yellow color.



of glycerol-/sorbitol-plasticized film with 5% ZnO NPs was significantly higher than the other treatments.

### SEM, XRD, FTIR, and TGA of Films

The cross-section morphology of the films was observed with SEM microscopy and presented in **Figure 2**. In general, sorbitol-plasticized films appeared to be more compact and denser than

glycerol-plasticized films. The film without the incorporation of ZnO NPs showed a rough structure and there were gaps in some parts of the film, while the addition of 3% ZnO NPs showed a fibrous and uneven film morphology, especially at the bottom of the film. However, the micrograph of the sorbitol-plasticized film reinforced by 5% ZnO NPs showed the film structure was even, homogeneous, and without pores and cracks.

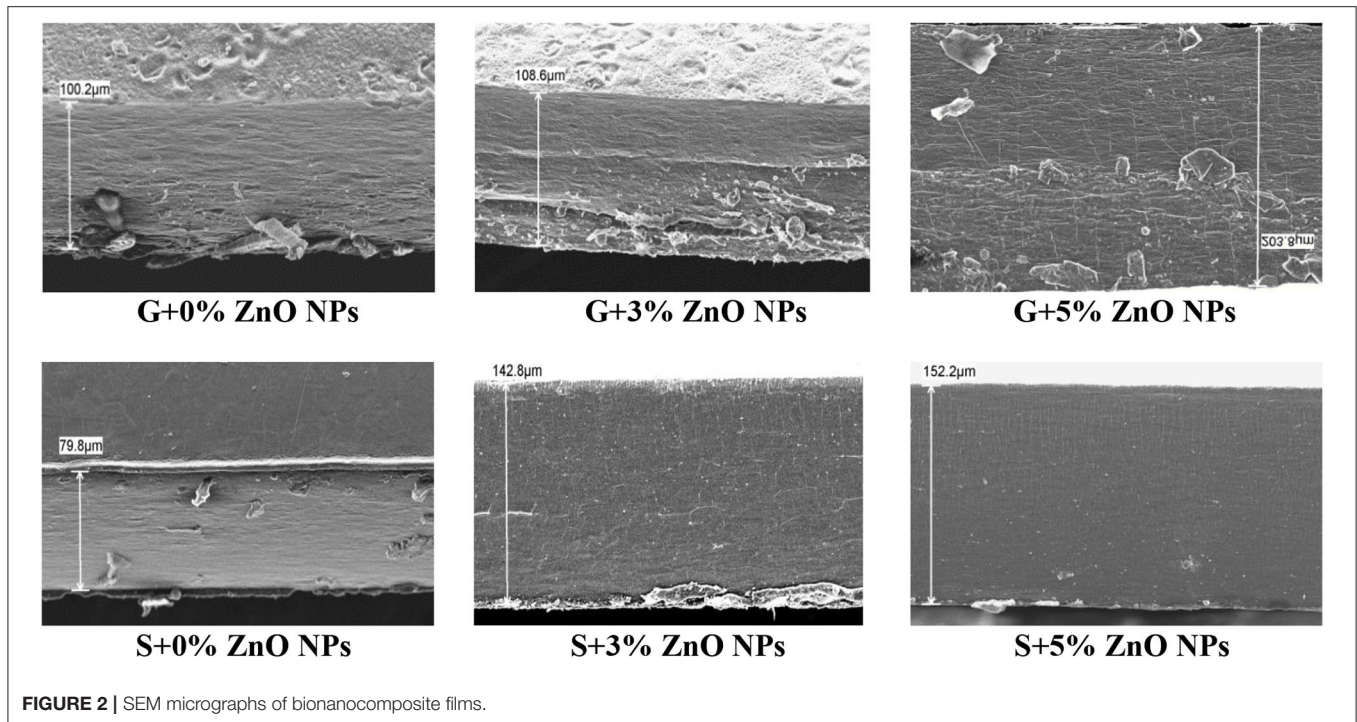


**FIGURE 2** | SEM micrographs of bionanocomposite films.

The X-ray diffraction pattern (XRD) of the film is presented in **Figure 3**. The sorbitol-plasticized film without the addition of ZnO NPs did not show any diffraction peaks on the XRD. However, the sorbitol-plasticized film reinforced by 3% and 5% ZnO NPs and the glycerol-plasticized film reinforced by 5% ZnO NPs showed some diffraction peaks. The sorbitol-plasticized films with 3% ZnO NPs showed diffraction peaks at  $2\theta = 34.87, 55.35, 61.45, 66, 58$ . The sorbitol-plasticized films with 5% ZnO NPs showed diffraction peaks at  $2\theta = 30.43, 33.11, 34.91, 46.23, 55.33, 61.59, 66.76$ . Beside, glycerol-plasticized films with 5% ZnO NPs showed diffraction peaks at  $2\theta = 31.74, 34.42, 36.23, 47.50, 56.51, 62.85, \text{ and } 67.94$ .

**Figure 4** showed that the spectrum of the film was in the range of  $3,462.93$  to  $567.41 \text{ cm}^{-1}$ . A typical broad absorption band with wavenumbers from  $3,429.85$  to  $3,462.93 \text{ cm}^{-1}$  was present in all the observed films. The glycerol-plasticized film with 3% ZnO NPs had a wavenumber of  $2,921.80$ . Meanwhile, in the plasticized film of glycerol and sorbitol with 5% ZnO NPs, new absorption bands were found in the  $2,310.45 \text{ cm}^{-1}$  and  $2,355.34 \text{ cm}^{-1}$  regions. In addition, the absorption band was found in the region  $2,145.27$  to  $2,166.43 \text{ cm}^{-1}$ . Furthermore, the absorption band was found in the region of  $1,629.14$  to  $1,635.08 \text{ cm}^{-1}$ . In addition, in the glycerol-plasticized film with 5% ZnO NPs and the sorbitol-plasticized film with 3% ZnO NPs, absorption bands appeared in the  $1,094.14$  and  $1,099.49 \text{ cm}^{-1}$  regions.

The thermogravimetric (TG) and derivative thermogravimetric (DTG) curves of the films are shown in **Figure 5**. All of the films exhibit the same degradation trend. The TGA and DTG curves clearly showed the onset degradation temperature ( $T_0$ ) and the maximum decomposition temperature ( $T_{\text{max}}$ ) of the film. In the first phase, all films began to degrade

at temperatures between  $37.52$  and  $172.80^\circ\text{C}$ . The sorbitol-plasticized film without the addition of ZnO NPs showed a  $T_0$  of  $243.40^\circ\text{C}$ , while the sorbitol-plasticized film with the addition of 5% ZnO NPs showed a  $T_0$  of  $249.91^\circ\text{C}$ . Furthermore, on the DTG curve, we could see that the  $T_{\text{max}}$  of the sorbitol-plasticized film without ZnO NPs was  $278.18^\circ\text{C}$ , while the sorbitol-plasticized film with the addition of 5% ZnO NPs had a higher  $T_{\text{max}}$  of  $281.92^\circ\text{C}$ .

## DISCUSSION

### Mechanical Properties

Based on **Table 1**, the tensile strength of sorbitol-plasticized film was significantly higher than the glycerol-plasticized film at all NCC concentrations. This was suspected due to hydrogen bonds being formed between starch-CMC-sorbitol-ZnO NPs than starch-CMC-glycerol-ZnO NPs. Sorbitol had a higher molecular weight ( $182.17 \text{ g/mol}$ ) than glycerol ( $\text{MW} = 92.094 \text{ g/mol}$ ), and consequently, more OH groups were formed which caused higher tensile strength (Kanmani and Rhim, 2014). In this study, the increased concentration of ZnO NPs was not significantly different in either glycerol- or sorbitol-plasticized films. This was presumably because the concentration of 3 and 5% ZnO NPs in this treatment resulted in the same distribution of nanomaterials in the polymer matrix. Gao et al. (2019) explained that ZnO nanoparticles could change the mechanical properties of film nanocomposites due to strong interfacial interactions between inorganic nanofillers and organic groups (starch matrix).

The ZnO NPs had a high surface area and surface energy, so if they are well-dispersed in the matrix, a strong surface

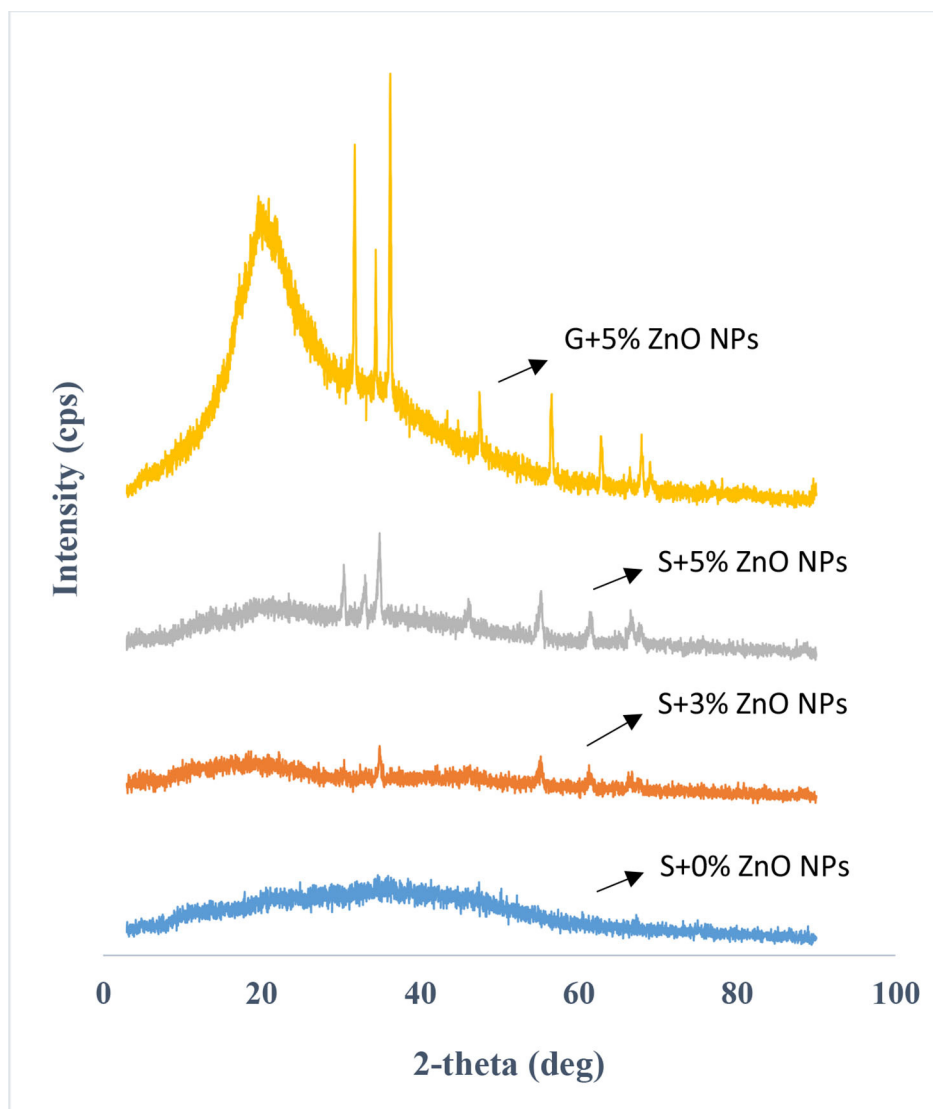


**FIGURE 3** | X-ray diffraction (XRD) of bionanocomposite films.

interaction will be generated between the ZnO nanoparticles and the matrix. Gao et al. (2019) stated that fillers and polymers were linked through static interactions, such as Vander Waals forces or Lewis acid–base interactions during physical mixing.  $Zn^{2+}$  on ZnO formed a salt bridge with a carboxylic group ( $COO^-$ ) and resulted in an interaction that improved the formation of the film structure. Vaezi et al. (2019) explained that the increase in mechanical properties was associated with the interaction between ZnO NPs and biopolymers because ZnO NPs could form hydrogen and covalent bonds with hydroxyl groups of starch, consequently strengthening the molecular strength between nanoparticles and biopolymers. In addition, hydrogen bonds formed between ZnO NPs and polymers could prevent nanoparticles from agglomeration. Agglomeration that occurs could reduce the strength of the interaction in the polymer

matrix. Therefore, the addition of ZnO NPs could increase the tensile strength of this film.

The elongation at the break value of the sorbitol-plasticized film with the addition of 5% ZnO NPs was significantly different from the others. The higher the concentration of added nanoparticles, the value of the percentage elongation at break increased, which indicated that the film was more elastic. This was in contrast to the statement of Torabi and Mohammadi Nafchi (2013), which stated that the addition of nanoparticles caused the contact of water and the matrix to be disturbed, resulting in reduced film elasticity. Therefore, the increase in the percentage of elongation was strongly influenced by the plasticizer of sorbitol. The addition of hydrophilic sorbitol into the starch matrix disrupted the hydrogen bonds between adjacent polymer molecules so that the intermolecular attraction strength

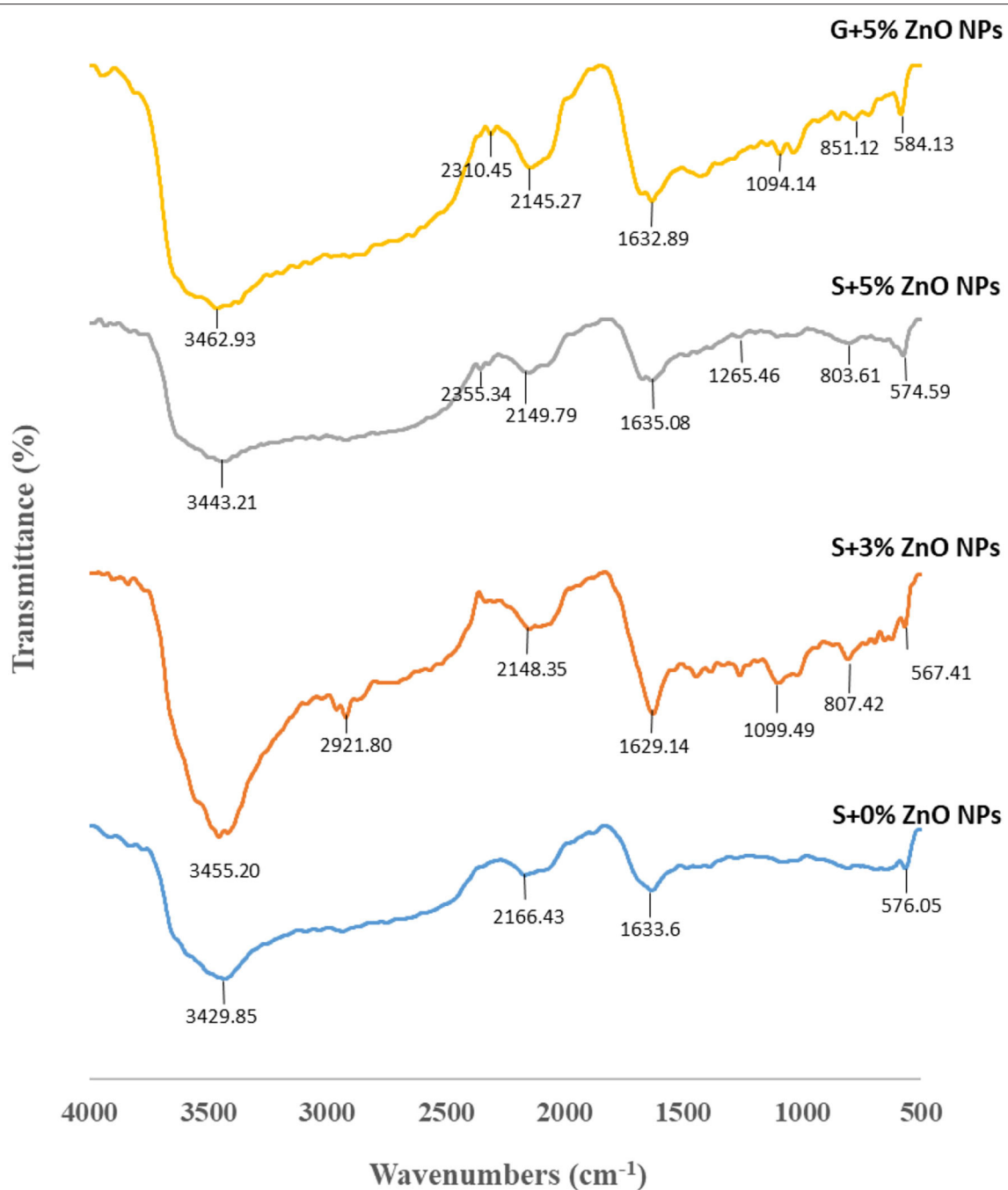


**FIGURE 4** | Fourier Transform Infrared (FTIR) spectra of the bionanocomposite films.

of the polymer chains was reduced, thereby increasing the flexibility and percent elongation of the film. The matrix in the film becomes less dense and allows polymer chain movement to occur when the film is stressed.

Young's modulus of sorbitol-plasticized film with the addition of 3 and 5% ZnO NPs was significantly higher than the film without ZnO NPs. This was presumably because ZnO NPs filled the polymer matrix and caused a strong bond

that made the film stiffer. **Table 1** showed that when the percent elongation increased, Young's modulus decreased. This was in accordance with Kramer (2009) that the modulus of elasticity was the inverse of the percentage elongation. If the percentage of elongation increased, the resulting modulus of elasticity decreased.

In general, the plasticizers of glycerol and sorbitol had more of a role in increasing the elongation at break value, while ZnO NPs



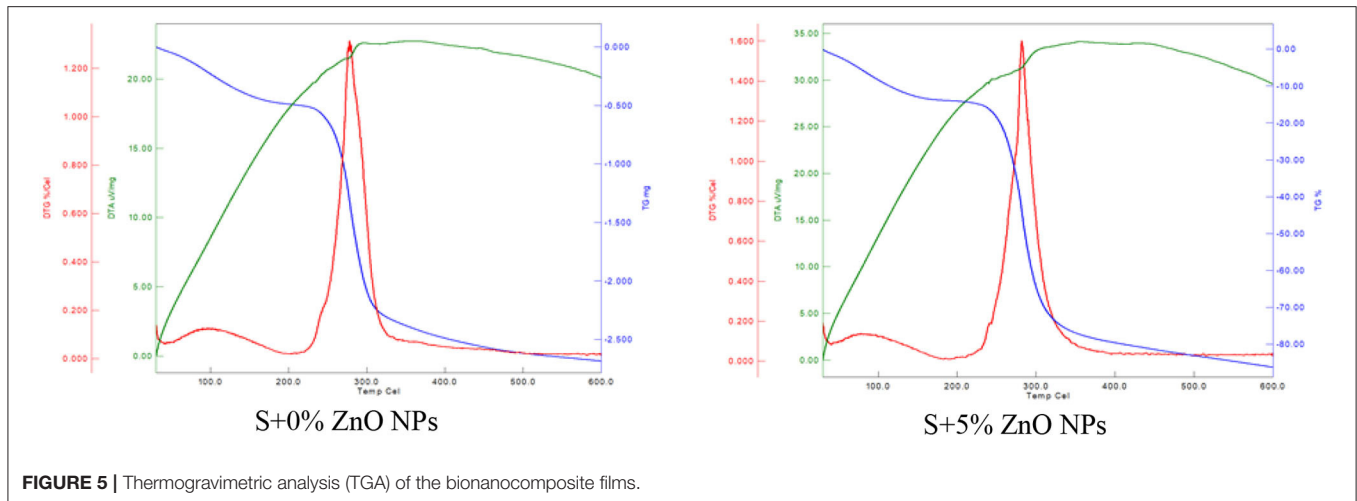


**FIGURE 5 |** Thermogravimetric analysis (TGA) of the bionanocomposite films.

had a greater role in increasing the tensile strength of the film, and Young's modulus of films was influenced by the plasticizer and ZnO NPs. In addition, the mechanical properties were also influenced by the type of corn starch and sorbitol. The use of corn starch as the base material for this film provides a solid structure for the film matrix. This was supported by Pramadita (2011) that polysaccharides could function in maintaining the compactness and stability of the film. The tensile strength of corn starch-based films was closely related to the presence of amylose and amylopectin where both the components play an important role in film formation. Amylose content of 29.96% in corn starch var. Paragon in the film plays a role in the compactness of the film, while the amylopectin content of 44.02% plays a role in the stability of the film. The heating process during film formation could weaken the hydrogen bonds in amylose so that gelatinization occurred, which continues with the diffusion of amylose and amylopectin. Amylose could form a strong gel in the retrogradation process, which was the result of combining starch polymers after the heating process.

### Water Vapor Transmission Rate

The amount of water vapor that passes through the surface of a nanocomposite film is WVTR. The higher the WVTR value, the more water vapor will enter the package or vice versa. The water vapor migration that occurs is generally in the hydrophilic part of the film so that the ratio between the hydrophilic and hydrophobic parts of the film component will affect the WVTR value of the film. The greater the hydrophobicity of the film, the smaller the WVTR value of the film (Panjaitan et al., 2019). WVTR is not only influenced by the filler but also by the filled compound (polymer matrix); the state of the matrix interface has an important role in determining the barrier properties of the nanocomposite films (Hu et al., 2019).

The WVTR of glycerol-plasticized films of 3 and 5% ZnO NPs were not significantly different, but those two treatments were significantly different from the WVTR of the film without the addition of ZnO NPs. This showed that the incorporation of nanofillers could reduce the WVTR value of the film. The

presence of ZnO NPs could reduce the rate of vapor transmission because they were solid and hydrophobic (Wahyu, 2014). The addition of nanoparticles could reduce the rate of water vapor transmission, and the barrier properties can be increased if the nanoparticles were well-dispersed in the matrix and had a high aspect ratio (Abdollahi et al., 2013). Nanoparticles made water vapor molecules go through a long and winding diffusion path (tortuosity) to pass and that made nanoparticles act as a barrier and reduce the rate of water vapor transmission (Vaezi et al., 2019).

Furthermore, in the sorbitol-plasticized film, the addition of 3 and 5% ZnO NPs was significantly different than without the addition of ZnO NPs. Among all of them, the higher significantly different WVTR values were found in sorbitol-plasticized film with 5% ZnO NPs. This was presumably because ZnO NPs could reduce the hollow space in the polymer matrix. The nanofiller could reduce the hollow space being oriented perpendicular to the diffusion path to a more compact nanoparticle–matrix network, which results in less space for water vapor to pass through (Hu et al., 2019; Vaezi et al., 2019). This was supported by Torabi and Mohammadi Nafchi (2013) that nanoparticles filled macromolecular or polymeric structures, which could reduce water vapor permeability. The addition of hydrophobic ZnO NPs was able to become a water vapor barrier in penetrating the film, and ZnO NPs were able to be dispersed in a polymer solution and act as a filler to reduce the water vapor permeability of the film. This was in line with Nafchi et al. (2012) where the addition of ZnO NPs could fill the macromolecular structure of polymers and significantly reduce water vapor permeability into polymer films based on sago starch and carrageenan.

### Water Solubility

The percentage of solubility of nanocomposite films is seen from the dry weight after being immersed in water for a certain time (Atef et al., 2014). The high solubility causes the nanocomposite film to be easily soluble in water and its ability to hold water is reduced.

In general, the treatment of all films with the incorporation of ZnO NPs was significantly lower than glycerol-plasticized films without ZnO NPs. This was presumably because the addition of ZnO NPs to the film matrix could strengthen the bonds in the film matrix so that it was not easily soluble in water. In addition, a higher concentration of nanoparticles added to the film solution could cause the solution molecules in the film matrix to increase so that the structure of the film network becomes more compact and sturdy. The strong film structure made the film not easily destroyed by water. This was in line with the research of Vaezi et al. (2019) who reported that the addition of ZnO NPs to the film resulted in the formation of more hydrogen bonds with matrix components. In addition, ZnO NPs showed excellent hydrophobic properties and so they were able to reduce the overall hydrophilic properties of the film. This was in line with Bajpai et al. (2010) who reported that ZnO nanoparticles in chitosan-based films were able to reduce the hydrophilic characteristics of the film, thereby reducing the solubility of the film in water.

The use of hydrophilic polymer materials, such as corn starch and glycerol or sorbitol plasticizers, in this study was not able to effectively resist the solubility of the film in water because corn starch and sorbitol were completely soluble in water. It is supported by Sobral et al. (2001) who reported that increasing the concentration of plasticizers increased the moisture content of the films due to the high hygroscopicity between adjacent macromolecules. Therefore, the presence of hydrophobic ZnO NPs filler could reduce the hydrophilic properties of the film, thereby reducing the water solubility of the film.

## Thickness

The thickness of the film is related to its ease of shaping. The thicker the film, the more rigid and difficult it is to form the film, but it will provide better mechanical protection for the food to be packaged. In general, the thickness of the glycerol-plasticized film was significantly higher than the sorbitol-plasticized film at any concentration of ZnO NPs. This was presumably because glycerol could increase the viscosity of the film solution so that when dried the film becomes thicker. In addition, glycerol-plasticized films with the addition of 3% and 5% ZnO NPs were not significantly different, but both were significantly different than without adding ZnO NPs. Meanwhile, the sorbitol-plasticized film with 5% ZnO NPs was significantly different from the addition of 0% and 3% ZnO NPs. This was because the addition of nanoparticles as a mixed film material could increase the thickness of the nanocomposite film. After all, it could act as a good filler. Chaichi et al. (2017) explained that nanoparticles had a large surface area and surface energy so that they could build strong interactions with the matrix and could be well-dispersed in the matrix. Furthermore, Anandito et al. (2012) reported that the increase in thickness could be caused by differences in the concentration of the film-making material, thereby increasing the total amount of dissolved solids in the film. This could increase the viscosity of the film solution which caused the film matrix after the drying process to become thicker.

## Film Color

The color of the nanocomposite film can affect the appearance of the packaged product. The  $L^*$  value of sorbitol/glycerol-plasticized film with the addition of 3 and 5% ZnO NPs was significantly lower than the sorbitol/glycerol-plasticized film without the addition of ZnO NPs. This was because the addition of nanoparticles to the film matrix could affect the brightness level of the resulting nanocomposite film. After all, the light on the surface of the nanoparticles would be reflected in smaller amounts, so the film was opaquer. This was in line with Nafchi et al. (2012), where the value of  $L^*$  will decrease significantly in the presence of zinc oxide nanoparticles. The mobility of polymer chains and the distance between molecules in the matrix affect the light permeability through the nanocomposite films (Afifah et al., 2018).

The value of  $a^*$  of the glycerol/sorbitol-plasticized film with 5% ZnO NPs was significantly higher than the other treatments. Increasing the concentration of ZnO NPs on the film would increase the  $a^*$  value of the film. This showed that the addition of ZnO NPs gave a red color to the film. The difference in color produced from the film with the addition of ZnO NPs showed that the color of the filler greatly affected the color of the resulting film. Following that the type of base material used will affect the color of the nanocomposite film.

Furthermore, the color value of  $b^*$  of the sorbitol-plasticized film with the incorporation of 5% ZnO NPs was significantly higher than the combination of 0 and 3% ZnO NPs. This was presumably because the ZnO NPs turn yellow when heated and the addition of ZnO NPs. This change occurs because some oxygen atoms were missing from the crystal lattice so that in a state of excess negative charge it produced a different color. The nanocomposite film solution with the addition of ZnO NPs, which was originally clear in color resulted in a yellowish nanocomposite film after the drying process in the oven. Besides, Vaezi et al. (2019) revealed that the addition of ZnO NPs changed the color of the film from bright white to bright yellow. The yellow color of the nanocomposite films with ZnO NPs was indicated by the  $b^*$  value, which tended to be higher than the nanocomposite films of other treatments. In accordance with Beak et al. (2017), the result of increasing the concentration of ZnO NPs on the film decreased the  $L^*$  value but increased the  $a^*$  and  $b^*$  values.

## Moisture Content

In general, the moisture content of glycerol-plasticized film was significantly different from the sorbitol-plasticized film. This was presumably because glycerol was more hydrophilic than sorbitol and presumably due to the higher molecular weight of sorbitol than glycerol. Meanwhile, sorbitol-plasticized films with the addition of 3 and 5% ZnO NPs had the highest significantly different water content than the others. This was presumably because the higher the concentration of added nanoparticles, the less the hydrophilicity of the film due to the hydrophobic ZnO NPs. The same result was reported by Tamimi et al. (2021), who explained that the decrease in moisture content was caused by a cohesive structure with high cohesion and less space and less hydrophilicity of ZnO NPs compared to starch-based matrices.

## SEM of Bionanocomposite Film

The cross-section morphology of the films was observed with SEM microscopy and presented in **Figure 2**. In general, sorbitol-plasticized films appeared to be more compact and denser than glycerol-plasticized films. It was suspected that sorbitol could facilitate a stable and strong interaction between the surface of ZnO NPs and the starch matrix compared to glycerol. In addition, the increase in the concentration of ZnO NPs resulted in a more even, compact, dense, and homogeneous film morphology. The film without the incorporation of ZnO NPs showed a rough structure and there were gaps in some parts of the film, while the addition of 3% ZnO NPs showed a fibrous and uneven film morphology, especially at the bottom of the film. However, the micrograph of the sorbitol-plasticized film reinforced by 5% ZnO NPs showed the film structure was even, homogeneous, and without pores and cracks. This was due to ZnO NPs being able to spread out and fill the empty spaces of the matrix well and interact better in the film matrix, resulting in a strong bond. According to Arifin et al. (2022), nanofillers could enter the basin area so that the surface becomes denser and homogeneous in the film matrix. Similar surface morphology was obtained by the addition of ZnO NPs into several other polymer films, such as ZnO–MMT–CS (Vaezi et al., 2019) and starch–PVA–ZnO NPs (Jayakumar et al., 2019).

## XRD of Bionanocomposite Film

The sorbitol-plasticized film without the addition of ZnO NPs did not show any diffraction peaks on the XRD diffractogram due to the amorphous nature of corn starch, where the crystalline portion of the starch was lost during the gelatinization of the film solution. However, the sorbitol-plasticized film reinforced by 3% and 5% ZnO NPs, and the glycerol-plasticized film reinforced by 5% ZnO NPs showed some diffraction peaks because ZnO NPs influenced the crystallinity of the film matrix. The sorbitol-plasticized films with 3% ZnO NPs showed diffraction peaks at  $2\theta = 34.87, 55.35, 61.45, 66,$  and  $58$  which corresponded to the diffraction plane of ZnO crystals (002), (110), (103), and (200), respectively. The sorbitol-plasticized films with 5% ZnO NPs showed diffraction peaks at  $2\theta = 30.43, 33.11, 34.91, 46.23, 55.33, 61.59,$  and  $66.76$ , which corresponded to the diffraction plane of ZnO crystals (100), (002), (002), (102), (110), (103), (200), and, respectively. Besides, glycerol-plasticized films with 5% ZnO NPs showed diffraction peaks at  $2\theta = 31.74, 34.42, 36.23, 47.50, 56.51, 62.85,$  and  $67.94$ , which corresponded to the diffraction plane of ZnO crystals (110), (002), (101), (102), (110), (103), and (112), respectively. This diffraction peak confirmed the presence of zinc oxide crystals in the film matrix. From the picture, it could be seen that the high concentration of ZnO NPs added to the film matrix caused higher diffraction peaks. Similar results were observed in several studies, such as Kanmani and Rhim (2014) and Vaezi et al. (2019).

## FTIR of Bionanocomposite Film

ATR-FTIR analysis was used to determine the functional groups and compounds formed between polymers, plasticizers, and ZnO NPs on bionanocomposite films. **Figure 4** showed that the spectrum of the film was in the range of  $3,462.93$  to  $567.41$   $\text{cm}^{-1}$ . A typical broad absorption band with wavenumbers from

$3,429.85$  to  $3,462.93$   $\text{cm}^{-1}$  was present in all the observed films. This was related to the presence of O-H bond strain vibrations. The incorporation of 3 and 5% ZnO NPs could increase the absorption intensity of the O-H group compared to films without the addition of ZnO NPs, thus confirming the increasing number of hydrogen bonds formed in the film matrix. Furthermore, the glycerol-plasticized film with 3% ZnO NPs had a wavenumber of  $2,921.80$   $\text{cm}^{-1}$ , and this was related to the stretching vibration of the C-H bond, while in the other treatments this bond was not confirmed. Meanwhile, in the plasticized film of glycerol and sorbitol with 5% ZnO NPs, new absorption bands were found in the  $2,310.45$  and  $2,355.34$   $\text{cm}^{-1}$  regions, which indicated the presence of C=N bonds. In addition, the absorption band was found in the region  $2,145.27$ – $2,166.43$   $\text{cm}^{-1}$ , which indicated the presence of C=C bonds. Furthermore, the absorption band was found in the region of  $1,629.14$ – $1,635.08$   $\text{cm}^{-1}$ , which indicated the presence of strong C = O bonds in the film. In addition, in the glycerol-plasticized film with 5% ZnO NPs and the sorbitol-plasticized film with 3% ZnO NPs, absorption bands appeared in the  $1,094.14$   $\text{cm}^{-1}$  and  $1,099.49$   $\text{cm}^{-1}$  regions, respectively, indicating the presence of C-O bonds in the film. The emergence of a new absorption band and a shift in the absorption band, as well as differences in absorption intensity from the FTIR results proved to indicate a new interaction that occurred between starch polymers with sorbitol/glycerol and ZnO NPs and the presence of ZnO vibrations recorded on the absorption band, thus affecting the characteristics of the bionanocomposite film. Similar results were found in other studies (Tamimi et al., 2021; Arifin et al., 2022).

## TGA of Bionanocomposite Film

In the first phase, all films began to degrade at temperatures between  $37.52$  and  $172.80^\circ\text{C}$ , and this was presumably due to the evaporation of water molecules in the film (Hu et al., 2019). Furthermore, the sorbitol-plasticized film without the addition of ZnO NPs showed a degradation temperature ( $T_0$ ) at  $243.40^\circ\text{C}$ , while the sorbitol-plasticized film with the addition of 5% ZnO NPs showed a higher  $T_0$  of  $249.91^\circ\text{C}$ . Furthermore, on the DTG curve, we can see that the  $T_{\text{max}}$  of the sorbitol-plasticized film without ZnO NPs was  $278.18^\circ\text{C}$ , while the sorbitol-plasticized film with the addition of 5% ZnO NPs had a higher  $T_{\text{max}}$  of  $281.92^\circ\text{C}$ . This was presumably because the presence of ZnO NPs in the film matrix could increase the thermal stability of the film due to the interaction between ZnO NPs and starch to prevent mass loss from the film. Kanmani and Rhim (2014) reported that the thermal stability of polymer films can be increased by the addition of ZnO NPs. In the second phase, it was suspected that there would be degradation of the organic functional groups of glycerol, starch, and CMC. Meanwhile, ZnO NPs-polymer film can be decomposed at higher temperatures. Similar results were found in previous studies (Kotharangannagari and Krishnan, 2016; Ponnamma et al., 2019).

## CONCLUSION

In this study, bionanocomposite films were developed using polymers from corn starch var. Paragon and CMC with the addition of plasticizer (glycerol or sorbitol) and the incorporation

of ZnO NPs. The higher the ZnO NPs added, the stronger the film because ZnO NPs were well-dispersed in the starch matrix. ZnO NPs had a reinforcing effect on the starch film, thereby increasing the tensile strength and decreasing the permeability of the film. However, the excess concentration of ZnO NPs could cause the film to be very stiff and reduce the barrier action of the film caused by the aggregation of ZnO NPs in the starch matrix. So, glycerol/sorbitol plasticizer was needed as a plasticizer that could increase the flexibility of the film. The compatibility between starch-CMC-plasticizer (glycerol/sorbitol)-and ZnO NPs significantly affected the mechanical properties, physical properties, and film permeability. Sorbitol-plasticized film with the incorporation of 5% ZnO NPs was the most optimum treatment among others because it had high tensile strength, elongation, and the lowest WVTR value. This film had the potential to be used as environmental friendly packaging and can be applied as food packaging.

## REFERENCES

- Abdollahi, M., Alboofetileh, M., Behrooz, R., Rezaei, M., and Miraki, R. (2013). Reducing water sensitivity of alginate bio-nanocomposite film using cellulose nanoparticles. *Int. J. Biol. Macromol.* 54, 166–173. doi: 10.1016/j.ijbiomac.2012.12.016
- Afifah, N., Sholichah, E., Indrianti, N., and Darmajana, A. D. (2018). Effect of plasticizer combination on edible film characteristics of carrageenan and beeswax. *Biopropal Indust.* 9, 49–60.
- Anandito, R. B. K., Nurhartadi, E., and Bukhori, A. (2012). *Effect of glycerol on the characteristics of edible film form Jali (Coix lacryma-jobi L.) flour.* 17–23.
- AOAC (2005). *Official Method of Analysis of the Association of Official Analytical Chemist.* Washington, DC: Benjamin Franklin Station.
- Arifin, H. R., Djali, M., Nurhadi, B., Hasim, S. A., Hilmi, A., and Puspitasari, A. V. (2022). Improved properties of corn starch-based bio-nanocomposite film with different types of plasticizers reinforced by nanocrystalline cellulose. *Int. J. Food Prop.* 25, 509–521. doi: 10.1080/10942912.2022.2052085
- ASTM (2002). "Standard test method for tensile properties of thin plastic sheeting (D882)," in *Annual Book of ASTM Standards.* Philadelphia, PA: American Society for Testing and Material.
- ASTM (2005). *Annual Book of ASTM Standards.* Philadelphia, PA: ASTM.
- Astuti, R. (2011). *Effect of Storage Time on Protein Content of Edible Film From Nata de Coco With Addition of Starch, Glycerin and Chitosan as Instant Noodle Seasoning Packaging.* Medan: Universitas Sumatera Utara.
- Atef, M., Rezaei, M., and Behrooz, R. (2014). Preparation and characterization agar-based nanocomposite film reinforced by nanocrystalline cellulose. *Int. J. Biol. Macromol.* 70, 537–544. doi: 10.1016/j.ijbiomac.2014.07.013
- Babaei-Ghazvini, A., Shahabi-Ghahfarrokhi, I., and Goudarzi, V. (2018). Preparation of UV-protective starch/kefir/ZnO nanocomposite as a packaging film: characterization. *Food Pack. Shelf Life* 16, 103–111. doi: 10.1016/j.fpsl.2018.01.008
- Bajpai, S. K., Chand, N., and Chaurasia, V. (2010). Investigation of water vapor permeability and antimicrobial property of zinc oxide nanoparticles-loaded chitosan-based edible film. *J. Appl. Polym. Sci.* 115, 674–683. doi: 10.1002/app.30550
- Beak, S., Kim, H., and Song, K., Bin. (2017). Characterization of an olive flounder bone gelatin-zinc oxide nanocomposite film and evaluation of its potential application in spinach packaging. *J. Food Sci.* 82, 2643–2649. doi: 10.1111/1750-3841.13949
- Chaichi, M., Hashemi, M., Badii, F., and Mohammadi, A. (2017). Preparation and characterization of a novel bionanocomposite edible film based on pectin and crystalline nanocellulose. *Carbohydr. Polym.* 157, 167–175. doi: 10.1016/j.carbpol.2016.09.062
- de Melo, C., Garcia, P. S., Grossmann, M. V. E., Yamashita, F., Dall'Antônia, L. H., and Mali, S. (2011). Properties of extruded xanthan-starch-clay nanocomposite films. *Braz. Arch. Biol. Technol.* 54, 1223–1333. doi: 10.1590/S1516-89132011000600019
- Febrianto Mulyadi, A., Hindun Pulungan, M., and Qayyum, N. (2016). Producing of cornstarch edible film and antibacterial activity test [the study of glycerol concentration and beluntas leaves extract (*Pluchea indica* L.)]. *Indust. J. Teknol. Manaja. Agroindust.* 5, 149–158. doi: 10.21776/ub.industria.2016.005.03.5
- Gao, W., Wu, W., Liu, P., Hou, H., Li, X., and Cui, B. (2019). Preparation and evaluation of hydrophobic biodegradable films made from corn/octenylsuccinated starch incorporated with different concentrations of soybean oil. *Int. J. Biol. Macromol.* 142, 376–383. doi: 10.1016/j.ijbiomac.2019.09.108
- Gontard, N., Guilbert, S., and Cuq, J.-L.-L. (1993). Water and glycerol as plasticizers affect mechanical and water vapor barrier properties of an edible wheat gluten film. *J. Food Sci.* 58, 206–211. doi: 10.1111/j.1365-2621.1993.tb03246.x
- Hu, X., Jia, X., Zhi, C., Jin, Z., and Miao, M. (2019). Improving the properties of starch-based antimicrobial composite films using ZnO-chitosan nanoparticles. *Carbohydr. Polym.* 210, 204–209. doi: 10.1016/j.carbpol.2019.01.043
- Isotton, F. S., Bernardo, G. L., Baldasso, C., Rosa, L. M., and Zeni, M. (2015). The plasticizer effect on preparation and properties of etherified corn starches films. *Industr. Crops Prod.* 76, 717–724. doi: 10.1016/j.indcrop.2015.04.005
- Jayakumar, A., Heera, K. V., Sumi, T. S., Joseph, M., Mathew, S., Praveen, G., et al. (2019). Starch-PVA composite films with zinc-oxide nanoparticles and phytochemicals as intelligent pH sensing wraps for food packaging application. *Int. J. Biol. Macromol.* 136, 395–403. doi: 10.1016/j.ijbiomac.2019.06.018
- JIS (1975). *Japanese International Standart 2 1707.* Tokyo: Japanese Standards Association.
- Kanmani, P., and Rhim, J. W. (2014). Properties and characterization of bionanocomposite films prepared with various biopolymers and ZnO nanoparticles. *Carbohydr. Polym.* 106, 190–199. doi: 10.1016/j.carbpol.2014.02.007
- Kotharangannagari, V. K., and Krishnan, K. (2016). Biodegradable hybrid nanocomposites of starch/lysine and ZnO nanoparticles with shape memory properties. *Mater. Des.* 109, 590–595. doi: 10.1016/j.matdes.2016.07.046
- Kramer, M. E. (2009). *Structure and Function of Starch-Based Edible Films and Coatings.* New York, NY: Springer. doi: 10.1007/978-0-387-92824-1\_4
- Liu, X., Chen, X., Ren, J., Chang, M., He, B., and Zhang, C. (2019). Effects of nano-ZnO and nano-SiO<sub>2</sub> particles on properties of PVA/xylan composite films. *Int. J. Biol. Macromol.* 132, 978–986. doi: 10.1016/j.ijbiomac.2019.03.088

## DATA AVAILABILITY STATEMENT

The original contributions presented in the study are included in the article/supplementary material, further inquiries can be directed to the corresponding author.

## AUTHOR CONTRIBUTIONS

All authors listed have made a substantial, direct, and intellectual contribution to the work and approved it for publication.

## ACKNOWLEDGMENTS

We gratefully thank the Internal Grant of Universitas Padjadjaran in Indonesia for financial support, the Unpad Doctoral Dissertation Research scheme (RDDU) no. 1427/UN6.3.1/LT/2020.

- Marta, H., Cahyana, Y., Arifin, H. R., and Khairani, L. (2019). Comparing the effect of four different thermal modifications on physicochemical and pasting properties of breadfruit (*Artocarpus altilis*) starch. *Int. Food Res. J.* 26, 269–276. doi: 10.1080/10942912.2019.1657447
- Marvizadeh, M. M., Oladzadabbasabadi, N., Mohammadi Nafchi, A., and Jokar, M. (2017). Preparation and characterization of bionanocomposite film based on tapioca starch/bovine gelatin/nanorod zinc oxide. *Int. J. Biol. Macromol.* 99, 1–7. doi: 10.1016/j.ijbiomac.2017.02.067
- Mohammadi Nafchi, A., Moradpour, M., Saeidi, M., and Alias, A. K. (2014). Effects of nanorod-rich ZnO on rheological, sorption isotherm, and physicochemical properties of bovine gelatin films. *LWT Food Sci. Technol.* 58, 142–149. doi: 10.1016/j.lwt.2014.03.007
- Montero, B., Rico, M., Rodríguez-Llamazares, S., Barral, L., and Bouza, R. (2017). Effect of nanocellulose as a filler on biodegradable thermoplastic starch films filled with nanorod-rich zinc oxide. *Carbohydr. Polym.* 157, 1094–1104. doi: 10.1016/j.carbpol.2016.10.073
- Nafchi, A. M., Alias, A. K., Mahmud, S., and Robal, M. (2012). Antimicrobial, rheological, and physicochemical properties of sago starch films filled with nanorod-rich zinc oxide. *J. Food Eng.* 113, 511–519. doi: 10.1016/j.jfoodeng.2012.07.017
- Nurhadi, B., Angeline, A., Sukri, N., Masruchin, N., Arifin, H. R., and Saputra, R. A. (2021). Characteristics of microcrystalline cellulose from nata de coco: hydrochloric acid versus maleic acid hydrolysis. *J. Appl. Polym. Sci.* 139, 1–12. doi: 10.1002/app.51576
- Panjaitan, N., Ulyarti, U., Mursyid, M., and Nazarudin, N. (2019). Modification of Yellow Uwi Starch (*Dioscorea alata*) Using the Precipitation Method and its Application for Edible film. *Andalas Agr. Technol. J.* 23. doi: 10.25077/jtpa.23.2.196-204.2019
- Ponnamma, D., Cabibihan, J. J., Rajan, M., Pethaiah, S. S., Deshmukh, K., Gogoi, J. P., et al. (2019). “Synthesis, optimization and applications of ZnO/polymer nanocomposites. *Mater. Sci. Eng. C* 98, 1210–1240. doi: 10.1016/j.msec.2019.01.081
- Pramadita, R. C. (2011). *Edible Film Characterization of Porang Flour (Amorphophallus oncophyllus) With the Addition Of Cinnamon (Cinnamon burmani) Essential Oil as Antibacterial*. Malang: Universitas Brawijaya, Malang.
- Sadegh-Hassani, F., and Mohammadi Nafchi, A. (2014). Preparation and characterization of bionanocomposite films based on potato starch/halloysite nanoclay. *Int. J. Biol. Macromol.* 67, 458–462. doi: 10.1016/j.ijbiomac.2014.04.009
- Schanda, J. (2007). *Colorimet Hoboken, New Jersey Understanding the CIE System*. Hoboken, NJ: John Wiley and Sons.
- Sobral, P. J. A., Menegalli, F. C., Hubinger, M. D., and Roques, M. (2001). Mechanical, water vapor marrier and thermal properties of gelatin based edible films. *Food Hydrocoll.* 15, 423–432. doi: 10.1016/S0268-005X(01)00061-3
- Tamimi, N., Mohammadi Nafchi, A., Hashemi-Moghaddam, H., and Baghaie, H. (2021). The effects of nano-zinc oxide morphology on functional and antibacterial properties of tapioca starch bionanocomposite. *Food Sci. Nutr.* 9, 4497–4508. doi: 10.1002/fsn3.2426
- Tavares, K. M., de Campos, A., Mitsuyuki, M. C., Luchesi, B. R., and Marconcini, J. M. (2019). Corn and cassava starch with carboxymethyl cellulose films and its mechanical and hydrophobic properties. *Carbohydr. Polym.* 223, 115055. doi: 10.1016/j.carbpol.2019.115055
- Torabi, Z., and Mohammadi Nafchi, A. (2013). The effects of SiO<sub>2</sub> nanoparticles on mechanical and physicochemical properties of potato starch films. *J. Chem. Health Risks* 3, 33–42. Available online at: [http://www.jchr.org/article\\_544018\\_e7d67303839505be12bd508e63eeb83e.pdf](http://www.jchr.org/article_544018_e7d67303839505be12bd508e63eeb83e.pdf)
- Vaezi, K., Asadpour, G., and Sharifi, H. (2019). Effect of ZnO nanoparticles on the mechanical, barrier and optical properties of thermoplastic cationic starch/montmorillonite biodegradable films. *Int. J. Biol. Macromol.* 124, 519–529. doi: 10.1016/j.ijbiomac.2018.11.142
- Wahyu, P. (2014). *Development of Bionanocomposite Film Based on Tapioca Starch and ZnO Nanoparticles with Glycerol Plasticizer*. Bogor: IPB.

**Conflict of Interest:** The authors declare that the research was conducted in the absence of any commercial or financial relationships that could be construed as a potential conflict of interest.

**Publisher’s Note:** All claims expressed in this article are solely those of the authors and do not necessarily represent those of their affiliated organizations, or those of the publisher, the editors and the reviewers. Any product that may be evaluated in this article, or claim that may be made by its manufacturer, is not guaranteed or endorsed by the publisher.

Copyright © 2022 Arifin, Djali, Nurhadi, Azlin-Hasim, Masruchin, Vania and Hilmi. This is an open-access article distributed under the terms of the Creative Commons Attribution License (CC BY). The use, distribution or reproduction in other forums is permitted, provided the original author(s) and the copyright owner(s) are credited and that the original publication in this journal is cited, in accordance with accepted academic practice. No use, distribution or reproduction is permitted which does not comply with these terms.